32nd URSI GASS, Montreal, 19-26 August 2017

Wireless Urban Propagation Measurements at 2.44, 5.8, 14.8 & 58.68 GHz

J. Medbo, D. Sundman, H. Asplund, N. Jaldén, and S. Dwivedi
Ericsson AB, SE-164 80 Stockholm, Sweden, https://www.ericsson.com

Abstract

This paper summarizes extensive wireless propagation measurements in an urban environment in Stockholm, Sweden. Effort has been put on ensuring comparability for all the different frequencies over the full range 2-60 GHz. Indoor office, outdoor-to-indoor, and outdoor street canyon scenario are investigated. Significant increase of propagation path loss with increasing frequency is observed for all these scenarios.

1. Introduction

The results reported herein are based on extensive wireless propagation measurements in the frequency range 2-60 GHz in and around an office building in an urban area of Stockholm. The main goal is to substantially improve the understanding of wireless propagation for 5G and IMT2020. Path loss characteristics in indoor (office), outdoor-to-indoor, and, urban street canyon scenarios have been investigated. Focus has been put on determining any frequency trends over the full measured frequency range. Similar studies have previously been reported in [1-3]. However, none of these studies were performed over such a large frequency range. Furthermore, comparing different measurement campaigns performed at different frequencies is not advisable as it is not possible to assess if any differences are caused by the different frequencies or by any other condition which is different for the different campaigns.

2. Measurement Set-Up

The setup used in the herein presented measurements is based on a vector network analyzer (VNA) and vertical dipole antennas which are matched for each frequency (2.44 GHz, 5.8 GHz. 14.8 GHz and 58.68 GHz,). This technique requires both ends of the radio link to be connected to the VNA by radio-frequency (RF) cables. In order to allow long range measurements, the RF signal is converted to an optical signal which is transmitted over a 300 m optical fiber and converted back to RF again. The corresponding signal loss over the fiber is negligible. For the 60 GHz measurements up- and down-converters are used in each end of the link.

3. Measurement Method and Data Processing

All conditions are carefully equalized to provide comparability between measurement data for the different frequencies. Particularly the measurement bandwidth, antenna patterns and dynamic power range are equal for all frequencies in all comparisons. This equalization is crucial in order to avoid fictitious frequency trends as pointed out in [4].

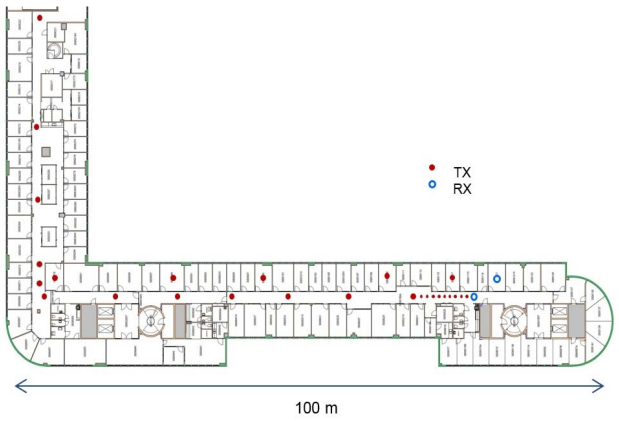

Figure 1. Floorplan of indoor office measurement scenario.

Most of the measurements are performed using vertical omni dipole antennas having very similar patterns for all frequencies. For the outdoor to indoor measurements vertical patch antennas or open waveguides are used at the outdoor transmitter location. Furthermore, the measurements performed around 60 GHz suffer from oxygen absorption of about 1.5 dB/100 m. As the measurements are wideband the delay information is obtained by Fourier transformation. The delay information is used for compensating propagation distance dependent additional loss at 60 GHz.

In order to facilitate assessment of any frequency dependent propagation effects, all measurement data is provided in terms of the loss in excess of free space loss. The excess loss is purely determined by propagation effects in contrast to free space loss for which the frequency dependence ($20\log f$) is a pure antenna aperture effect. For this purpose, all measurement data is carefully calibrated by line of sight (LOS) short range (0.1-1.0 m) measurements.

4. Indoor Office Measurements

The basic indoor layout (See Figure 1) is a corridor with office rooms along both sides. At the end of the corridor there is a 90 degrees turn. The receive (RX) antenna is

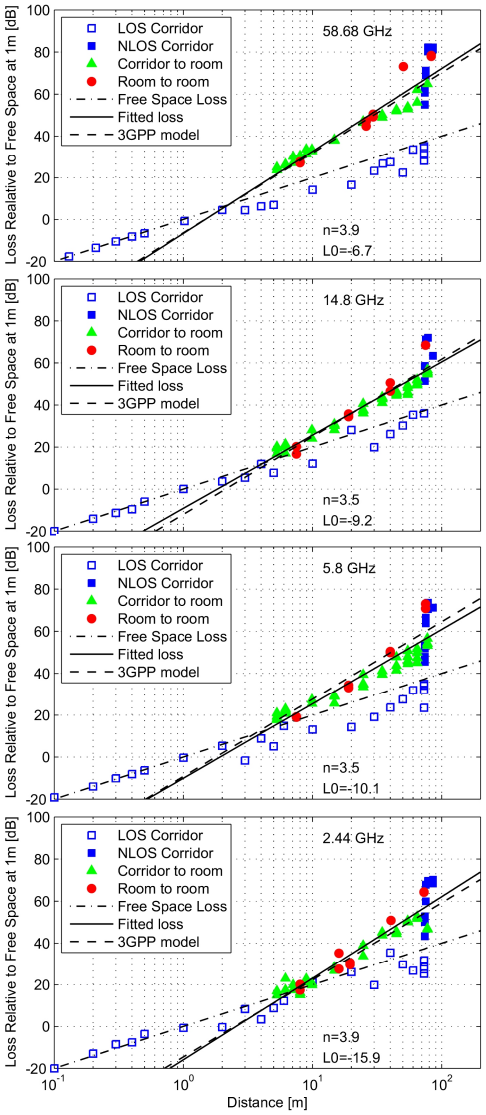

Figure 2. Path loss, in excess free space loss, versus distance for 2.44, 5.8, 14.8 and 58.68 GHz measured in the indoor office environment.

placed at two locations, one in the corridor and one inside an adjacent office room. The transmit antenna is placed at different locations both in the corridor and inside office rooms. The exterior walls of the building are made of brick and the interior walls of plasterboard and glass.

Figure 2 summarizes the main results of the path loss analysis. The loss, L, relative to free space power at one meter distance is plotted for the frequencies, 2.44 GHz, 5.8 GHz. 14.8 GHz and 58.68 GHz, for the different LOS and NLOS scenarios. It should be noted that the additional loss due to oxygen absorption at 58.68 GHz has been compensated for. A two parameter exponent model

$$L = 10n\log_{10}(d) + L_0 \text{ [dB]} \qquad (1)$$

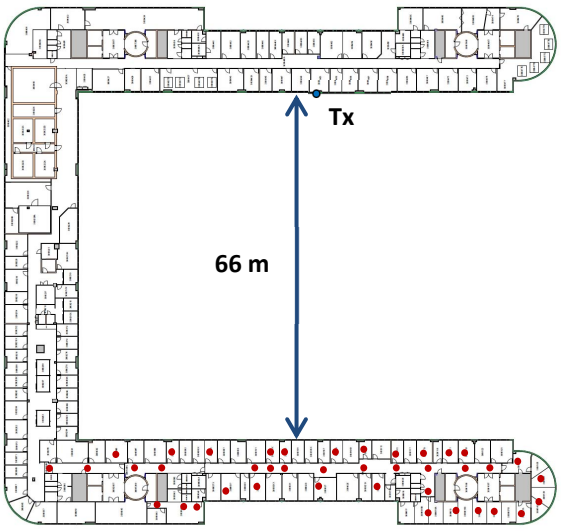

Figure 3. Outdoor to indoor measurement scenario. The indoor Rx locations are marked with red filled circles and the Tx location is marked with a blue filled circle.

has been fitted to the measurement data where d is the distance between transmitter and receiver in meters. The corresponding model by 3GPP [5] accounts also for the frequency dependence

$$L_{3gpp} = 38.3\log_{10}(d) + 17.3 + 24.9\log_{10}(f) \text{ [dB]} \quad (2)$$

where f is the carrier frequency in GHz. It is clear from the figure that the measurement data agree very well with the 3GPP model. There is clear frequency trend as the propagation loss increases about 5 dB per decade in addition to the free space loss.

5. Outdoor to Indoor Measurements

An outdoor-to-indoor multi-frequency measurement campaign has been performed in an eight stores tall office building in Kista, Stockholm as depicted in Figure 3. The transmitter is located in an open window at the top floor of the building and the received signal is measured at 2 slightly shifted (30 cm) positions at 40 indoor locations across the inner yard on the same floor. At the top floor of the building the exterior wall is covered with metal. The windows are however pure glass without metallization.

Between 2.44 GHz and 14.8 GHz the building penetration loss ranges from around 0 dB up to 30 dB (Figure 4). The lower end of penetration loss around 0 dB is similar for all frequencies while the highest losses around 45 dB occurs only at 58.68 GHz. The minimum loss, due to penetration of the exterior wall/window only, is in the range 0-5 dB with the highest values for 5.8 GHz and 58.68 GHz. This non-monotonic dependence on frequency may be explained assuming that the three layers of glass, in the

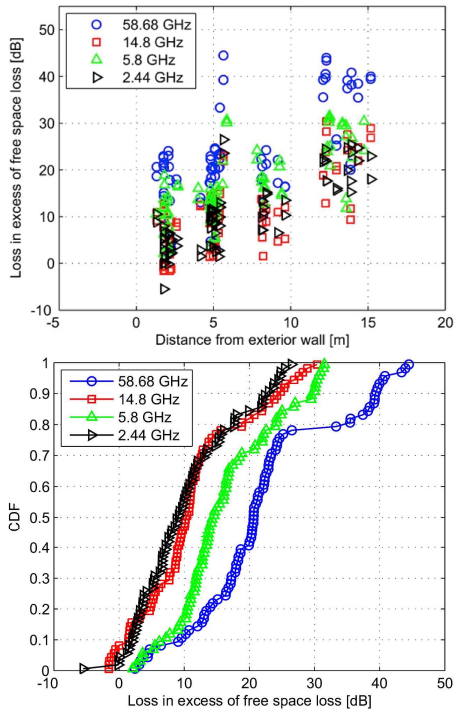

Figure 4. Measured outdoor to indoor loss, in excess of free space loss, for the different frequencies. In the upper graph the loss as function of distance from the exterior wall, which is in LOS with respect to the transmitter, is shown, and, in the lower graph the CDFs are shown.

window frames, cause constructive or destructive interference, as an effect of multiple reflections, resulting in periodic varying attenuation as function of frequency. Subsequent measurements show that the window loss is about 2, 10, 0, and, 6 dB at 2.44, 5.8, 14.8 and 58.68 GHz respectively which confirms this effect and explains the measured minimum penetration loss. Moreover, it is clear that the spread of penetration loss is substantially larger for the higher frequencies. This may partly be the result of the venetian blinds, in some of the windows, which block the vertically polarized waves at the higher frequencies but are transparent at the lower frequencies. The measurement results agree very well with corresponding 3GPP model [5].

6. Outdoor Street Canyon Measurements

Outdoor measurements are made in an urban area consisting of mainly modern office building blocks of about 100 m length and 25 m height and about 20 m street width (Figure 5). The measurements are performed in both LOS and NLOS in a street canyon with receiver RX1 located on a bridge at about 5 m above ground and receiver RX2 located about 1.5 m above ground level. In both transmitter routes (TX routes in Figure 5), the antenna height is 1.5 m. In Figure 5 the excess loss is shown for all frequencies. In LOS a multipath gain of up to 5 dB is observed which is similar at all frequencies. This gain is due to additional paths from reflections off the ground and

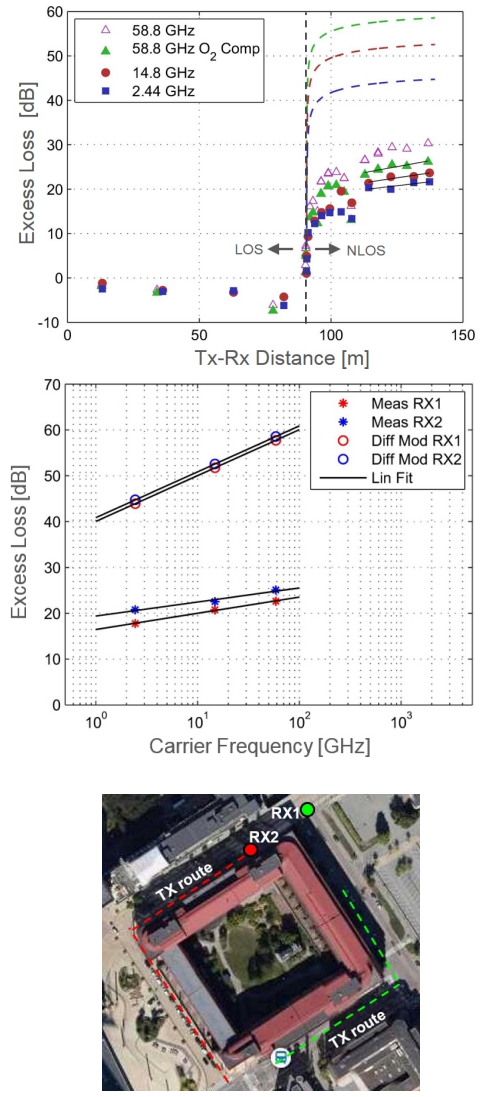

Figure 5. Measured loss versus distance for RX2 (upper graph) for the scenario shown in the lower graph. Corresponding loss by knife edge diffraction is marked with dashed lines. In the middle graph, the excess loss versus frquency are shown for both measurements and knife edge diffraction together with linear fits.

exterior walls. In the NLOS region behind the corner of the building a substantial increase in the excess loss is observed. This loss is substantially lower than what would be expected by knife edge diffraction only, at the corner, as indicated in Figure 5. Further, the frequency dependence is much weaker than what is expected from diffraction. This result suggests that the dominating propagation mechanisms in NLOS must be other than diffraction, e.g. specular and/or diffuse scattering by objects or rough exterior walls. Moreover, it is clear that the oxygen compensation at 60 GHz is substantial, up to 4 dB, for the NLOS data which is more than what is expected from the link distance only. This is, however, explained by that the lengths of significant reflected propagation paths are substantially larger than the link distance. The frequency dependence of measured excess loss and corresponding

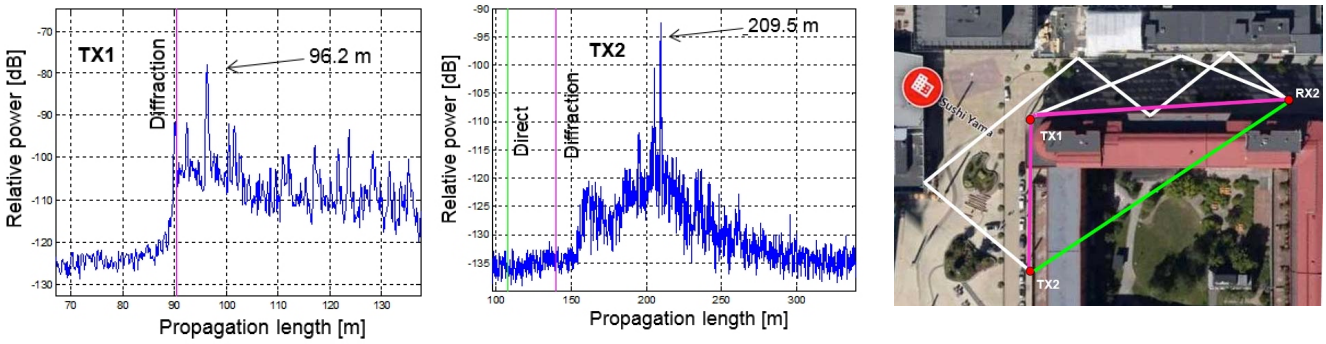

Figure 6. Power delay profiles in NLOS locations TX1 and TX2 at 60 GHz and corresponding reconstructed pathways.

knife edge diffraction model [6] are shown in Figure 6. The measured frequency dependence of excess loss ($\sim 3 \log f$ [dB]) is clearly less than what expected by knife edge diffraction ($\sim 10 \log f$ [dB]). This result is in agreement with the frequency dependency of the 3GPP channel model for high frequencies reported in [5].

In order to get some further insight into the propagation mechanisms, manual ray-tracing has been performed for two measurement locations at 60 GHz as shown in Figure 6. The first transmitter location (TX1) is in NLOS but very close to LOS. The first arriving path is attenuated by diffraction. The pathway of the strongest path was possible to reconstruct assuming one specular reflection off an exterior building wall along the street. The second transmitter location (TX2) is substantially further down the street into the NLOS region. At the delay corresponding to the diffraction path around the corner no signal above the noise floor is observed. The first cluster of weak paths is observed at substantially longer propagation distances than the diffraction path length. This cluster is likely to be caused by scatterers and/or rough surfaces in the area of the street corner. The strongest peak stands out having around 20 dB higher power level than the rest of the power delay profile. This path was possible to reconstruct assuming four specular reflections off exterior building walls showing that specular paths may be important even far into the NLOS region. However, for most of the NLOS locations such pronounced peaks were not observed.

7. Summary

Extensive wireless propagation measurements, have been performed in the frequency range 2-60 GHz in an urban environment in Stockholm, Sweden. The results of a thorough analysis show that the propagation path loss increases significantly with frequency in all measured scenarios, particularly in the outdoor to indoor scenario. For the outdoor street canyon scenario, it is, though, shown that this increase may not be explained by diffraction. It is more likely that the main propagation mechanisms, in NLOS, are scattering by rough surfaces or small objects as well as specular reflection. This would also explain why the measured increase in path loss with frequency is substantially smaller than what is expected by diffraction. Furthermore, all reported results are in agreement with the 3GPP channel model for higher frequencies [5].

8. Acknowledgements

The research leading to these results received funding from the European Commission H2020 programme under grant agreement no 671650 (mmMAGIC project). The authors would like to acknowledge the contributions of their colleagues in mmMAGIC, although the views expressed are those of the authors and do not necessarily represent the project. Further the authors would like to acknowledge Martin Furuskog who contributed substantially in performing the measurements.

7. References

1. T. S. Rappaport, F. Gutierrez, E. Ben-Dor, J. N. Murdock, Y. Qiao, & J. I. Tamir, (2013). "Broadband millimeter-wave propagation measurements and models using adaptive-beam antennas for outdoor urban cellular communications," IEEE transactions on antennas and propagation, 61(4), 1850-1859.

2. M. Inomata, W. Yamada, M. Sasaki, M. Mizoguchi, K. Kitao, & T. Imai, (2015). "Path loss model for the 2 to 37 GHz band in street microcell environments." IEICE Communications Express, 4(5), 149-154.

3. 5GCM White Paper, "5G Channel Model for bands up to 100 GHz," Dec 2015. (http://www.5gworkshops.com/) .

4. J. Medbo, N. Seifi, H. Asplund, "Frequency dependency of measured highly re-solved directional propagation channel characteristics", European Wireless, 2016

5. 3GPP TR 38.900 V14.1.0 "3rd Generation Partnership Project; Technical Specification Group Radio Access Network; Study on channel model for frequency spectrum above 6 GHz (Release 14)," Tech. Rep., 2016.

6. J. Medbo, F. Harrysson, (2013, April). "Channel modeling for the stationary UE scenario," In Antennas and Propagation (EuCAP), 2013 7th European Conference on (pp. 2811-2815). IEEE.